Theor Chem Acc (2012) 131:1116
DOI 10.1007/s00214-012-1116-z

REGULAR ARTICLE

Comparative study on the Al–Al multiple bond in $Na_2[Arx'AlAlArx']$ and $H_2[Arx'AlAlArx']$ ($Arx' = C_6H_3$-2, 6-$(C_6H_5)_2$)

Xiaoyan Li · Jie Sun · Lingpeng Meng · Yanli Zeng · Shijun Zheng

Received: 10 October 2011 / Accepted: 8 December 2011 / Published online: 4 February 2012

Abstract The Al–Al multiple bond in $Na_2[Arx'AlAlArx']$ ($Arx' = C_6H_3$-2,6-$(C_6H_5)_2$) was investigated and compared with $H_2[Arx'AlAlArx']$ by electron localization function (ELF) method. The roles of sodium, hydrogen atoms, and bulky ligands in these two complexes were also discussed. The calculated results show that $Na_2[Arx'AlAlArx']$ and $H_2[Arx'AlAlArx']$ have different structural and electronic features. In $Na_2[Arx'AlAlArx']$, the Al–Al bond includes a σ bond, a normal π bond and a slipped π bond. In $H_2[Arx'AlAlArx']$, the direct Al–Al bond was substituted by two 3-center, 2-electron (3c–2e) bridged bonding, which formed by the hydrogen and two aluminum atoms. The bulky ligands play important stabilizing roles in both $Na_2[Arx'AlAlArx']$ and $H_2[Arx'AlAlArx']$.

Keywords Al–Al bond · Hydrogen bridged bond · Topological analysis of electron density · Electron localization function

1 Introduction

In 1988, Uhl and co-workers reported the synthesis of a novel compound, R_2AlAlR_2 (R=$CH(SiMe_3)_2$), as the first example of a stable molecule with an Al–Al bond to be structurally characterized [1]. This compound marked a key development for compounds with Group 13 metal–metal bonds [2]. Soon afterwards, numerous molecules which contain double or triple bonds which were previously thought unable to exist have been synthesized [3–11]. Since 2006, the first "dialumunene" species $Na_2[Ar'AlAlAr']$ ($Ar' = C_6H_3$-2, 6-$(C_6H_3$-2, 6-$iPr_2)_2$) was been synthesized by Power and co-workers. X-ray crystallographic analysis of $Na_2[Ar'AlAlAr']$ revealed a centrosymmetric Al_2Na_2 core with Al–Al and Al–Na separations of 2.4281 and 3.1521 Å, respectively, and the C–Al–Al–C array has a *trans*-bent structure (C–Al–Al dihedral: 131.72°) with local C_{2h} symmetry [2].

A. J. Bridgeman discussed the Al–Al bond for several model compounds, $[Al_2R_2]^{2-}$, $Li_2[Al_2R_2]$ (R=H, Me and Ph) using hybrid density functional theory. The presence of the lithium atoms does not greatly change the geometry of the $M_2H_2^{2-}$ fragment but does act to stabilize the out of plane π bonding orbital and reduce the M–M bond order [12]. H. J. Himmel calculated the reaction enthalpies for Al–Al bond in $[HAlAlH]^{2-}$ and $Na_2[HAlAlH]$ [13]. The results show that the presence of the sodium ions has a significant impact on the chemistry and thus suggests that they are involved to a large extent in the bonding. However, some people think that the model systems are too simple to influence the properties of metal–metal bond [14].

In this study, the nature of Al–Al bonding in $Na_2[Arx'AlAlArx']$ and $H_2[Arx'AlAlArx']$ ($Arx' = C_6H_3$-2,6-$(C_6H_5)_2$) was investigated and compared within the framework of the 'atoms in molecules' (AIM) [15, 16] theory and using electron localization function' (ELF) [17–19] analysis. With comparison, the similarities and differences of electronic structures and bond characteristics of two molecules have been studied. The roles of sodium, hydrogen atoms, and bulky ligands in these two complexes are also discussed.

X. Li · J. Sun · L. Meng · Y. Zeng · S. Zheng (✉)
College of Chemistry, Institute of Computational Quantum Chemistry, Hebei Normal University, Yuhua Road, Shijiazhuang 050016, China
e-mail: sjzheng@mail.hebtu.edu.cn

2 Computational details

The hybrid density functional B3LYP has proven to be an accurate method for reproducing the metal–ligand bond lengths, particularly metal–metal bond distances [20]. Thus, the geometries of the studied complexes were optimized using density functional theory (DFT) at the B3LYP/6-311G (d, p) levels using the Gaussian 03 program package [21].

A detailed topological analysis of electron density was made according to AIM theory, as proposed by Bader [15, 16], using the program AIMALL [22]. The ELF topological analysis was performed using the TopMod [23, 24] suite of programs using a rectangular parallelepiped grid of points and a step size of 0.025 Bohr, the two-dimensional ELF are plotted by Multiwfn [25]. For both the AIM and ELF studies, the wave functions were calculated at the B3LYP/6-311G (d, p) level. The bonding characteristics were analyzed by natural bond orbital (NBO) theory [26] using the NBO package included in the Gaussian 03 suite of program.

3 Results and discussion

3.1 $Na_2[Arx'AlAlArx']$

3.1.1 Equilibrium geometry

According to the experimental results [2], the original symmetry of $Na_2[Arx'AlAlArx']$ ($Arx' = C_6H_3$-2,6-$(C_6H_5)_2$) is defined as C_{2h}. The geometry of $Na_2[Arx'AlAlArx']$ was calculated. The optimized geometry is shown in Fig. 1, and the structural parameters are given in Table 1, along with the experimental values.

As shown in Fig. 1a, the $Na_2[Arx'AlAlArx']$ molecule has a *trans*-bent geometry, in which two sodium atoms reside on either side of the Al–Al bond, forming a nearly planar Al_2Na_2 ring. This geometry is similar to that of the experimental structure of $Na_2[Ar'AlAlAr']$ ($Ar' = C_6H_3$-2,6-$(C_6H_3$-2,6-$i Pr_2)_2$), only lacking the isopropyl substituents. The calculated Al–Al bond length in $Na_2[Arx'AlAlArx']$ is 2.4650Å, and the Al–Na and Al–C bond lengths are 3.1182 and 2.0901 Å, respectively. The bond angle of Al–Al–Na is 66.7°. All of the parameters are very close to the experimental parameters [2]. The results mean that our calculated level is suitable for the complexes studied.

3.1.2 AIM analysis

According to AIM theory [15, 16], a chemical structure is represented by a network of bond paths. The presence of a bond path provides a universal indicator of the bonding that exists between the linked atoms.

Figure 1b presents the molecular graph of $Na_2[Arx'AlAlArx']$. It can be seen that there is a bond critical point (BCP) located at the midpoint of two aluminum atoms and two bond paths link the BCP to these two aluminum atoms. Considering the sodium atoms, a conflict structure exists in which the sodium atoms are linked by the bond path to the BCP of the Al–Al bond, not to the aluminum atoms.

The topological data from the BCP calculation for the Al–Al bond, such as the values of the electron density $\rho(r)$, the Laplacian of the electron density $\nabla^2\rho(r)$ and the total energy density H_c (the sum of the Lagrangian kinetic density G_c and the virial energy density V_c of $Na_2[Arx'AlAlArx']$), are collected in Table 2. The values of $\rho(r)$ and $\nabla^2\rho(r)$ at the BCP of the Al–Al bond are 0.0047 a.u. and −0.0355 a.u., respectively; the value of H_c for the Al–Al bond is −0.0179 a.u. For the Al–Al bond, the value of $\rho(r)$ is surprisingly low for a homonuclear shared interaction, compared to values ranging from 0.14 a.u. for boron–boron single bond to 0.77 a.u. for the nitrogen–nitrogen triple bond [27]. $\nabla^2\rho(r)$ is close to zero, being slightly negative for the formal single bond. The values of the energy density H_c are negative. The low values of electron density $\rho(r)$ at the BCP of the metal–metal bond as well as for the H_c make classification of the metal–metal bond using only AIM criteria somewhat

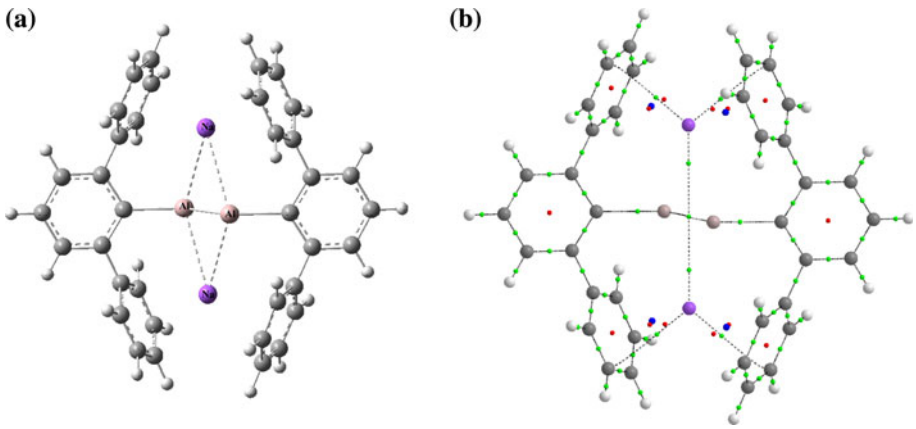

Fig. 1 Geometry (**a**) and molecular graph (**b**) of $Na_2[Arx'AlAlArx']$

Table 1 The calculated geometry parameters and experimental values of Na_2[Arx′AlAlArx′] and H_2[Arx′AlAlArx′]

	Na_2[Arx′AlAlArx′]		H_2[Arx′AlAlArx′]
	Calculated value	Experimental value[b]	Calculated value
BL(Al–Al)[a]	2.4650	2.4281	2.5846
BL(Al–Na/H)	3.1182	3.1521	1.7347
BL(Al–C)	2.0901	2.0432	2.0025
A(Al–Al–Na/H)	66.7	67.7	41.8
A(Al–Na/H–Al)	46.6	45.4	96.3
A(C–Al–Al)	123.6		131.1
D(Al–Na/H–Al–Na/H)	0.0		0.0
D(C–Al–Cl–C)	180.0		180.0

[a] *BL* bond length, in angstrom; *A* bond angle, in degree; *D* dihedral angle, in degree

[b] The experimental value comes from reference [2]

Table 2 Topological properties at the BCPs of Na_2[Arx′AlAlArx′]

	Al–Al	Na-(AlAl)	Na–C	Al–C
ρ(r)	0.0447	0.0155	0.0050	0.0645
$\nabla^2\rho$(r)	−0.0355	0.0253	0.0204	0.2065
H_c	−0.0179	−0.0007	0.0010	−0.0161

All values in a.u.

ambiguous. This circumstance has been already pointed out for other metal–metal bonding in transition metal complexes [28–32].

Furthermore, there are BCPs located between the sodium atoms and terphenyl ligands, which means that there exist interactions between sodium atoms and terphenyl ligands. From Table 2, the electron density ρ(r) at the BCP of Na–C bond is 0.0050, it does fall within the prosed range of 0.0020–0.0160 a.u. for weak bond [33, 34]; the positive $\nabla^2\rho$(r) and H_c at the BCP of Na–C bond are positive, and according to Bader's [35] and Cramer's criteria [36], these interactions belong to non-convalent interactions. These non-convalent weak interactions play important stabilizing roles to shelter the reactive M–M bonds in the studied complexes.

3.1.3 ELF analysis

It is well-known that multiple M–M bonds are too reactive to be isolated unless protected from attack by bulky ligands that shelter them. It is generally believed that these bulky ligands play a passive role, serving only to shelter the reactive M–M bonds, but not otherwise altering the essential structural and electronic features of the molecule [37]. The complexity of the terphenyl ligands makes the use of ELF methods for the study of Na_2[Arx′AlAlArx′] molecule difficult [38]. Therefore, to make computation more convenient, Na_2[PhAlAlPh] was chosen as the model molecule to analyze the nature of the Al–Al bond. In this model molecule, the bond length of the Al–Al bond and the bond angle of Al–Na–Al are restricted to those in Na_2[Arx′AlAlArx′].

The two-dimensional ELF contours and three-dimensional ELF iso-surfaces of Na_2[PhAlAlPh] are shown in Fig. 2, and the calculated results for the ELF analysis are collected in Table 3. The ELF calculation yields the core basin of aluminum and sodium atoms, with values 10.0e. The calculated population of C(Na) corresponds to the $(1\ s)^2(2s2p)^8$ sequence of electrons for Na^+. As shown in Fig. 2, two aluminum atoms and two sodium atoms are contained in a quarter-synaptic basin. The total population in the quarter-synaptic valence basins is equal to 5.77e. This results in the sodium atoms to lose 2e and provide Al–Al bonding. Compared with the classical C≡C triple bond in acetylene, the total population is smaller than 6e. This means the strength of the Al–Al bond is close to while weaker than the triple bond.

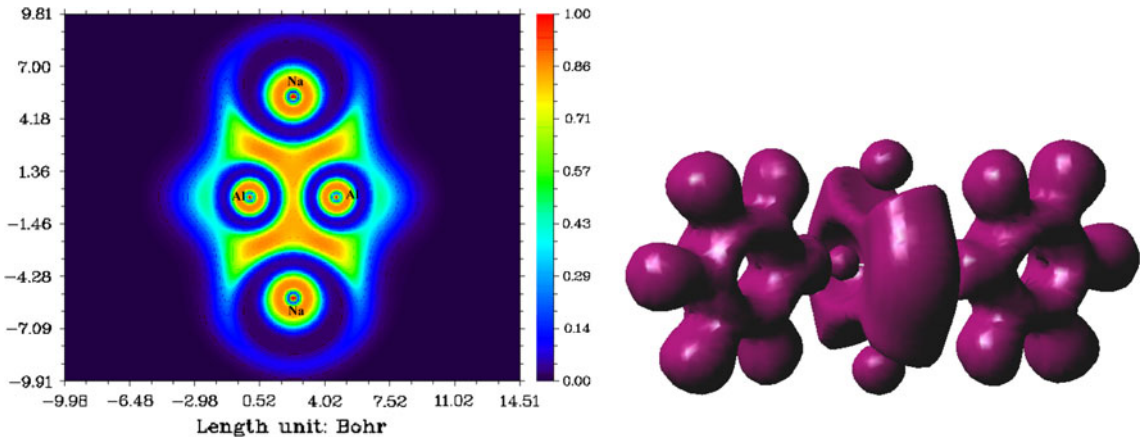

Fig. 2 Two-dimensional (2D) cross-sections through the molecules and three-dimensional (3D) representation ELF of the Na_2[PhAlAlPh]

Table 3 The population in various basin of Na_2[PhAlAlPh]

C(Al1)	C(Al2)	C(Na1)	C(Na2)
9.96	9.96	10.02	10.02
V(Al1,Na1,Na2)	V(Al1,Al2,Na1)	V(Al2,Na1,Na2)	V(Al1,Al2,Na2)
2.63	0.23	2.64	0.27

As shown in Fig. 2, the Al–Al bonding is characterized by a ring-shaped region of localized electrons. The shape of valence basin means the bonding region of Al–Al bond is more than the double bond domains of ethene, and the shape of valence basin is similar to the triple bond domains of ethyne [39]. However, there are some differences between them. In ethyne, the ring-shaped region of localized electrons is regular, while in Na_2[PhAlAlPh], the ring is not very regular, since the top and bottom of the ring is "thinner" than other parts. This shape indicates that the Al–Al bonding is stronger than the normal double bond while weaker than the normal triple bond. It can be classified as a non-classical triple bond.

3.1.4 NBO analysis

The natural bond orbital (NBO) analysis reveals that there are three Al–Al bond orbitals in Na_2[Arx′AlAlArx′], as shown in Fig. 3, one Al–Al σ bond and two π bond (a normal π bond and a slipped π bond) orbitals, the electron occupancy of these three orbital is 1.7150, 1.8178 and 1.6619, respectively. The σ bond orbital involves 25.92% s and 73.98% p character, the normal π molecule orbital is purely composed of the p orbital of aluminum atoms, the slipped π bond orbital is not located on the midbond plane, symmetrically above and below the nuclear axis but is instead precisely at the positions expected for two lone pairs, one on each aluminum. The NBO analysis further confirms the charge distribution on sodium atom is +0.6187, indicated that the two sodium atoms as a electron donor in Na_2[Arx′AlAlArx′]. The NBO analysis on orbital is supportive of the intriguing Al–Al triple bond and consistent with the above discussions.

3.2 H_2[Arx′AlAlArx′]

3.2.1 Equilibrium geometry

The H_2[Arx′AlAlArx′] molecule is optimized with C_{2h} symmetry with the geometry shown in Fig. 4.

The geometry of H_2[Arx′AlAlArx′] is similar to that of Na_2[Arx′AlAlArx′], which also has a *trans*-bent geometry,

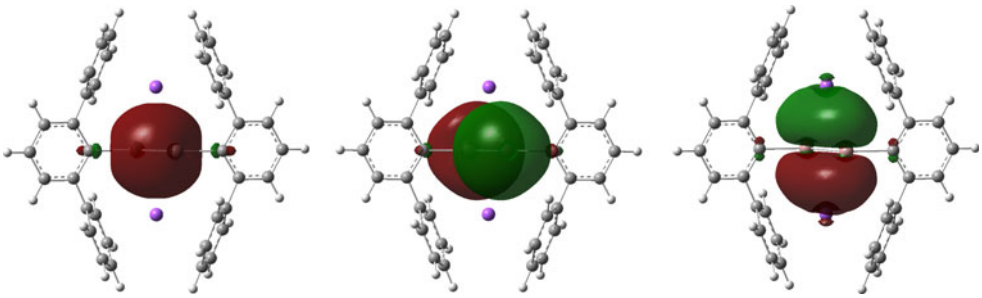

Fig. 3 Natural bond orbitals of the Na_2[Arx′AlAlArx′]

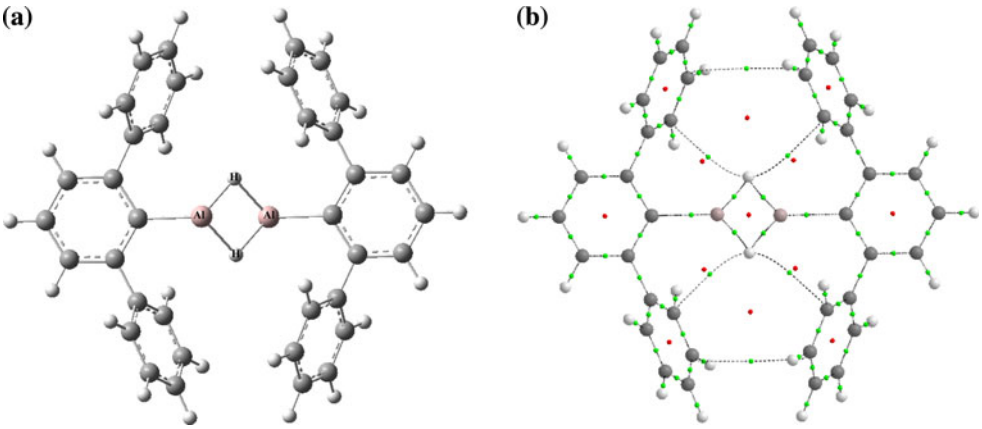

Fig. 4 Geometry (**a**) and molecular graph (**b**) of H_2[Arx′AlAlArx′]

with two hydrogen atoms residing on either side of the Al–Al bond, forming a nearly planar Al_2H_2 four-membered ring, the detailed geometric parameters are also listed in Table 1. Compared to Na_2[Arx′AlAlArx′], the Al–H bond length is 1.7347 Å and the length of the Al–Al bond in H_2[Arx′AlAlArx′] is 2.5846 Å, which is longer than that of the Al–Al bond in Na_2[Arx′AlAlArx′] (2.4650 Å). The C–Al–Al–C chain is bent. The Al–Al–C angle is calculated to be 131.1°, which is larger than that found in Na_2[Arx′AlAlArx′]. In addition, the H_2[Arx′AlAlArx′] molecule has a Al–H–Al bridged structure with a Al–H–Al angle of 96.3°, which is larger than the Al–Na–Al angle in Na_2[Arx′AlAlArx′] (46.6°).

3.2.2 AIM analysis

Figure 4 also presents a molecular graph of H_2[Arx′AlAlArx′]. As shown in Fig. 4b, no bond critical point (BCP) exists between the aluminum atoms, the BCP exist between aluminum and hydrogen atoms, and the bond paths link aluminum atoms and hydrogen atoms. That is, the multi-center Al–H–Al bonding presents in H_2[Arx′AlAlArx′], and the two aluminum and two hydrogen atoms form a nearly planar Al_2H_2 four-membered ring. Furthermore, there are weaker interactions present between the two terphenyl ligands. These interactions also contribute to the shorter Al–Al bond.

The properties of BCP, that is, the values of the electron density ρ(r), the Laplacian of the electron density $\nabla^2\rho$(r) and the energy density H_c and the delocalization index δ(A, B), are collected in Table 4.

Table 4 Topological properties at the BCPs in H_2[Arx′AlAlArx′]

	ρ(r)	$\nabla^2\rho$(r)	H_c
Al–H	0.0573	0.1514	−0.0156
Al–C	0.0777	0.2557	−0.0255

All values in a.u.

As shown in Table 4, the values of the Laplacian of the electron density $\nabla^2\rho$(r) are positive and the energy density H_c are negative for the Al–H and Al–C bonds. These reveal that the Al–H and Al–C bonds are covalent interactions. The Al–C bond is a normal single bond. The electron density ρ(r) and the delocalization index δ(Al, H) of Al–Al bond are smaller than those of the Al–C bond, which indicates that the strength of the Al–H bond in the Al–H–Al bridged structure is weaker than a normal single bond.

Meanwhile it can be seen that there are bond critical points (BCPs) located between the hydrogen atom and carbon atom of the phenyl groups, as well as the carbon atom of the phenyl group and carbon atom of the opposite phenyl group, which mean that there are interactions between the hydrogen atom and the terminal phenyl group on each Arx′, as well as one phenyl group and the other phenyl group. These weak interactions, similar as those in Na_2[Arx′AlAlArx′], shelter the reactive M–M bonds and play important stabilizing roles in the studied complexes.

3.2.3 ELF analysis

The nature of the bonding in H_2[Arx′AlAlArx′] has also been studied using a topological analysis of the ELF. For convenient computational purposes, we report the analysis of the Al–Al bonding in the model molecules H_2[PhAlAlPh].

The 2D plots of the ELF for H_2[PhAlAlPh] are shown in Fig. 5. As was seen from Fig. 5, two aluminum atoms and bridging hydrogen atoms are contained in the same basin. The 3D ELF iso-surface ($\eta = 0.5$) for H_2[PhAlAlPh] is shown in Fig. 5. There is a ring-shaped region of localized electrons, which consists of two monosynaptic basins V(Al) and two trisynaptic basins V(Al–H–Al). The valence basins are characterized by the number of core basins with which they have a boundary. The C(Al) core basin population equals 9.96e. The monosynaptic basins correspond to electron lone pairs, disynaptic basins to conventional two-center bonds, and trisynaptic basins to 3c–2e bonds [40]. In addition, the V(Al–H–Al) basin population equals 2.02e,

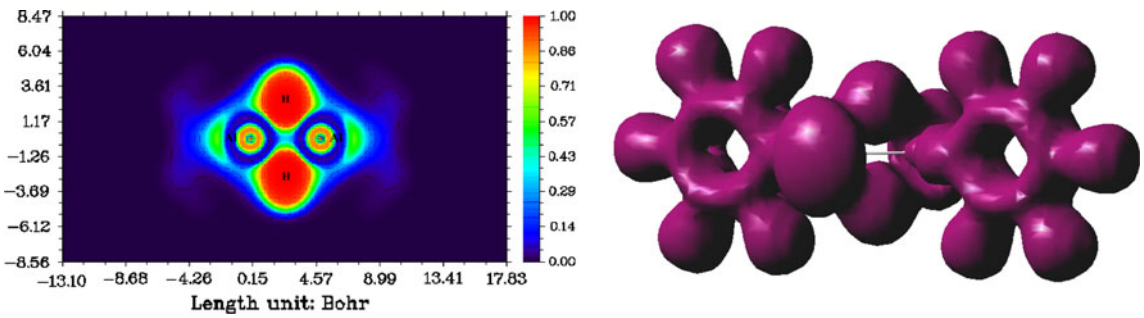

Fig. 5 Two-dimensional (2D) cross-sections through the molecules and three-dimensional (3D) representation of the election localization function (ELF) for H_2[PhAlAlPh]

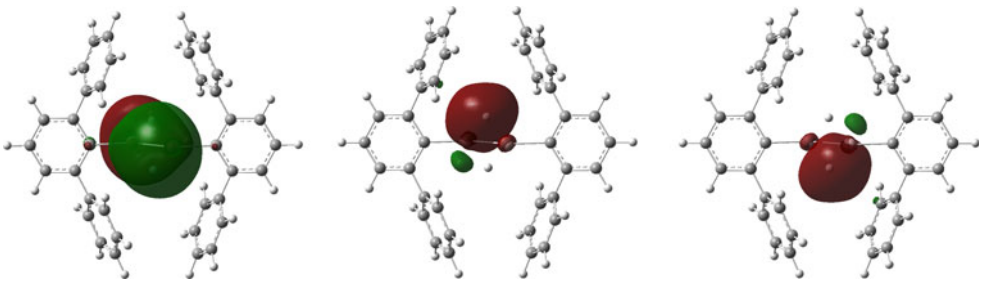

Fig. 6 Natural bond orbitals of the H_2[Arx′AlAlArx′]

therefore the Al–H–Al bond is a hydrogen bridge bond (3c–2e bond). The V(Al) basins appear as monosynatic basins rather than disynaptic V(Al, Al). They are not located on the midbond plane, symmetrically above and below the axis but instead precisely at the positions expected for two lone pairs, one on each aluminum atom.

3.2.4 NBO analysis

The 3c–2e bond structure is also convinced by the results of NBO analysis. The NBO analysis on H_2[Arx′AlAlArx′] (Fig. 6) shows that there are two Al–H–Al bridge bonds that substitute the Al–Al σ bond and normal π bond in Na_2[Arx′AlAlArx′]; the Al–H–Al bridge bond is composed by the s(33.33%), p(65.02%) orbitals of aluminum atoms and the s(99.80%) orbital of hydrogen atom; the composition of orbital means that the sp^2 hybrid of aluminum atom overlapping with the s orbital of hydrogen atom forms the Al–H–Al bridge bond; in another word, the hydrogen atom participates in covalent interaction, and the charge distribution on aluminum and hydrogen atom is 1.0437 and −0.4173, respectively. Furthermore, there are three valence electrons in aluminum atom, one electron participates the formation of the Al–C covalent bond with the bulky ligand and the other two are contributed to form two Al–H–Al bridged bonds. Therefore, the Al–Al σ and normal π bonding in Na_2[Arx′AlAlArx′] are replaced by the two Al–H–Al bridged bonds in H_2[Arx′AlAlArx′].

4 Conclusions

The Al–Al bonding in Na_2[Arx′AlAlArx′] and H_2[Arx′AlAl Arx′] has been discussed and compared. The analyses carried out in this work lead to the following main features:

(1) The calculated results indicate that the molecules Na_2[Arx′AlAlArx′] and H_2[Arx′AlAlArx′] have different structural and electronic features.
(2) The Al–Al bond in Na_2[Arx′AlAlArx′] is a non-classical triple bond, which consists of a σ bond, a normal π bond and a slipped π bond. Its strength is greater than a normal double bond but weaker than a normal triple bond.
(3) In the H_2[Arx′AlAlArx′] molecule, there are two 3c–2e (Al–H–Al) bonds and each of the aluminum atoms contributes one electron.
(4) In Na_2[Arx′AlAlArx′], two sodium atoms act as the electron donor while hydrogen atoms participate in the covalent interaction in H_2[Arx′AlAlArx′]; the bulky subsistents play important stabilizing roles in both Na_2[Arx′AlAlArx′] and H_2[Arx′AlAlArx′].

Acknowledgments This work was supported by the National Natural Science Foundation of China (Contract No: 20973053, 21073051, 21102033, 21171047), the Natural Science Foundation of Hebei Province (Contract No. B2010000371, B2011205058) and the Education Department Foundation of Hebei Province (ZD2010126).

References

1. Uhl WZ (2008) Naturforsch B 43:1113–1118
2. Wright RJ, Brynda M, Power PP (2006) Angew Chem Int Ed 45:5953–5956
3. Power PP (1998) J Chem Soc: 2939–2951 (trans: Dalton)
4. Power PP (1999) Chem Rev 99:3463–3504
5. Weidenbruch MJ (2002) Organomet Chem 646:39–52
6. Uhl W (1997) Coord Chem Rev 163:1–32
7. Uhl W (1998) Rev Inorg Chem 18:239–282
8. Linti G, Schnöckel H (2000) Coord Chem Rev 206:285
9. Schnöckel H, Schnepf A (2001) Adv Organomet Chem 47:235–281
10. Robinson GH (1999) Acc Chem Rev 32:773–782
11. Weidenbruch M (2003) Angew Chem 115:2322–2324; Angew Chem Int Ed 42:2222
12. Bridgeman AJ, Ireland LR (2001) Polyhedron 20:2841–2851
13. Himmel HJ, Schnöckel H (2002) Chem Eur J 8:2397–2405
14. Takagi N, Schmidt MW, Nagase S (2001) Organometallics 20:1646–1651
15. Bader RFW (1990) Atoms in molecules-a quantum theory. Oxford University Press, Oxford
16. Popelier P (2000) Atoms in molecules: an introduction. UMIST, Manchester
17. Becke AD, Edgecombe KE (1990) J Chem Phys 92:5387–5403
18. Silvi B, Savin A (1994) Nature 371:683–686
19. Savin A, Nesper R, Wengert S, Fassler T (1997) Angew Chem Int Ed Engl 36:1808–1832
20. Sorkin A, Truhlar DG, Amin EA (2009) J Chem Theory Comput 5:1254–1265
21. Frisch MJ, Trucks GW, Schlegel HB et al (2004) Gaussian 03, revision D.01. Gaussian, Inc., Wallingford, CT
22. Keith TA (2010) AIMAll. Version 10(05):04
23. Noury S, Krokidis X, Fuster F, Silvi B (1997) TopMod package, Paris

24. Noury S, Krokidis X, Fuster F, Silvi B (1999) Comp Chem 23:597–604
25. Lu T (2011) Multiwfn: a multifunctional wavefunction analyzer, version 2.1.2, http://Multiwfn.codeplex.com
26. Reed AE, Curtiss LA, Weinhold F (1988) Chem Rev 88:899–926
27. Molina JM, Dobado JA, Heard GL, Bader RFW, Sundberg MR (2001) Theor Chem Acc 150:365–373
28. Andrés J, Berski S, Feliz M, Llusar R, Sensato F, Silvi B (2005) C R Chimie 8:1400–1412
29. Savin A, Nesper R, Wengert S, Fässler T (1997) Angew Chem Int Ed Engl 36:1808–1832
30. Bianchi R, Gervasio G, Marabello D (2000) Inorg Chem 39:2360–2366
31. Macchi P, Proserpio DM, Sironi A (1998) J Am Chem Soc 120:13429–13435
32. Bianchi R, Gervasio G, Marabello D (1998) Chem Commun 15:1535–1536
33. Sanz P, Yanez M, Mó O (1998) J Phys Chem A 106:4661–4668
34. Hazra AB, Pal S (2000) J Mol Struct (Theochem) 497:157–163
35. Bader RFW (1990) Atoms in molecules: a quantum theory. Clarendon, Oxford
36. Cremer D, Kraka E (1984) Angew Chem Int Ed Engl 23:627–628
37. Cotton FA, Cowley AH, Feng XJ (1998) J Am Chem Soc 120:1795–1799
38. Macchia GL, Gagliardi L, Power PP, Brynda M (2008) J Am Chem Soc 130:5104–5114
39. Grützmacher H, Fässler TF (2000) Chem Eur J 6:2317–2324
40. Silvi B (2002) J Mol Struct 4614:3–10